Journal of
Materials Chemistry B

Materials for biology and medicine

Accepted Manuscript

This article can be cited before page numbers have been issued, to do this please use: M. Verma, M. Chaudhary, A. Singh, N. Kaur and N. Singh, *J. Mater. Chem. B*, 2020, DOI: 10.1039/D0TB01195A.

This is an Accepted Manuscript, which has been through the Royal Society of Chemistry peer review process and has been accepted for publication.

Accepted Manuscripts are published online shortly after acceptance, before technical editing, formatting and proof reading. Using this free service, authors can make their results available to the community, in citable form, before we publish the edited article. We will replace this Accepted Manuscript with the edited and formatted Advance Article as soon as it is available.

You can find more information about Accepted Manuscripts in the Information for Authors.

Please note that technical editing may introduce minor changes to the text and/or graphics, which may alter content. The journal's standard Terms & Conditions and the Ethical guidelines still apply. In no event shall the Royal Society of Chemistry be held responsible for any errors or omissions in this Accepted Manuscript or any consequences arising from the use of any information it contains.

ROYAL SOCIETY OF CHEMISTRY

rsc.li/materials-b

View Article Online
DOI: 10.1039/D0TB01195A

ARTICLE

Naphthalimide – Gold based Nanocomposite for the Ratiometric Detection of Okadaic Acid in Shellfish

Received 00th January 20xx,
Accepted 00th January 20xx

DOI: 10.1039/x0xx00000x

Meenakshi Verma,[a†] Monika Chaudhary,[b†] Amanpreet Singh,[c] Navneet Kaur,[d,*] Narinder Singh[c,*]

Okadaic acid (OA) is one of the known marine biotoxin produced by various dinoflagellates and exists in sea food such as shellfish. The consumption of contaminated shellfish with OA leads to diarrheic shellfish poisoning (DSP) which results in inhibition of protein phosphatases enzymes in humans. This poisoning can cause immunotoxicity and tumor promotion due to accumulation of okadaic acid more than allowed limits in bivalve molluscs. The reported methods for the detection of okadaic acid include mouse bioassays, immunoassays, chromatography coupled with spectroscopic techniques, electrochemical and immunosensors etc. We have developed naphthalimide-gold based nanocomposite for the detection of Okadaic acid. Individually, the organic nanoparticles (ONPs) of synthesized naphthalimide based receptor and gold coated ONPs are less sensitive for detection. However, the fabrication of the composite of Au@ONPs and ONPs enhances the sensing properties and selectivity. The composite shows ratiometric response in UV-Vis absorption spectrum and quenching in fluorescence profile with limit of detection 20 nM for OA in aqueous medium. In cyclic voltammetry, a shift was observed in cathodic peak (-0.532 V to -0.618 V) as well as in anodic peak (-0.815 V to -0.847 V) on addition of Okadaic Acid. To study quick binding of composite with OA time response experiment was performed. Also, the developed sensor retains its sensing ability in pH range of 5-9 and high salt effects. Our developed composite can be used for the detection of OA in real applications.

Introduction

Toxins are natural secondary metabolites usually produced by microorganisms, fungi, animals or plants, are endangering food, water resources and human health.[1] Owing to their carcinogenic and mutagenic nature these mycotoxins can adversely affect the functioning of kidney, liver, gastrointestinal tract, nervous system and blood-vascular system. Mycotoxins also causes damages to the reproductive function and leads to hormonal imbalance.[2] These mycotoxins consist of diverse substances having molecular weight ranging from 0.14 kDa to 150 kDa.[3] However, the toxicity rely on many factors e.g. quantity, application, and the particular mode of action within the organism. Existence of such toxic materials makes them strong candidates that can be used as biological warfare agents and exhibit a risk for human beings.[4-5] Food and water containing traces of mycotoxins can seriously endanger the public health. Food such as cereals, fruits, wines etc, generally contains mycotoxins. The marine toxins exist in the sea food such as shellfish.[6] Food contamination may diversely effect agriculture and food industry and also it may affect economic, production and recreational areas (e.g. agricultural and shellfish industry). These pollutants can enter the chain from agricultural activities (pesticides/herbicides), side products from industries, pharmaceutical compounds (drugs/antibiotic), terrorists and military activities (explosives molecules)[7] or toxins produced by aquatic animals or phytoplankton blooms.[8-9]

Marine toxins form an interesting group of complex organic compounds having long-lasting impact on human beings. The increased emergence of toxins is a possible result of raised ocean temperature that promotes algal blooms. On the basis of their chemical structure, point of origin and characteristics these can be classified into six groups. These groups include (i) diarrheic shellfish poisoning (DSP, mainly due to okadaic acids and dinophysistoxins), (ii) paralytic shellfish poisoning (PSP, due to saxitoxins), (iii) amnesic shellfish poisoning (ASP, due to domoic acids), (iv) neurotoxic shellfish poisoning (NSP, due to brevetoxins) (v) azaspiracid poisoning (AZP, due to azaspiracids), and (vi) ciguatera fish poisoning (CFP, due to ciguatoxins).[10] However, their increasing level in warming marine environment necessitates considerable monitoring of toxins in sea products.[11]

Diarrheic shellfish poisoning (DSP) is caused by consumption of okadaic acid (OA) contaminated shellfish by human beings. The main symptoms of DSP in humans are vomiting,

[a] Department of UCRD, Chandigarh University, Ghraun, Mohali, - 140413, India
[b] Centre for Biomedical Engineering, Indian Institute of Technology Ropar, Roopnagar, Punjab-140001, India
[c] Department of Chemistry, Indian Institute of Technology Ropar, Roopnagar, Punjab-140001, India
[d] Department of Chemistry, Panjab University, Chandigarh – 160014, India.
† Equal Contribution

Electronic Supplementary Information (ESI) available: [details of any supplementary information available should be included here]. See DOI: 10.1039/x0xx00000x

abdominal pain, nausea and diarrhea.[12-13] Okadaic acid (OA) is a well-known marine toxin which is produced by algae of the genera Dinophysis and Prorocentrum.8 It is a lipophilic as well as heat-stable phycotoxin which can accumulate in different types of shellfish, generally in scallops, mussels, oysters and clams.[14] Inhibition of protein phosphatases, PP1 and PP2A enzymes is supposed to be the reason of toxicity of OA.[15,16] According to the European Union, 160 μg of OA per kg is the highest allowed limit in the bivalve molluscs.[17] Higher than this allowed limit of OA may lead to immunotoxicity and tumor promotion.[18] Hence, OA contaminated shellfish is not only harmful for human health but also for shellfish industry, worldwide. Thus, development of detection methods for OA is need of the time. Till 2011, the traditional method for the detection of OA, the mouse bioassay was utilized as suggested by European Commission (EC). However, mouse bioassay had some drawbacks associated with it such as low selectivity, sensitivity, inconvenience of usage and time consumption.[19,20] Therefore, EC recommended other methods such as protein phosphatase inhibition assays or immunoassays,[21] chromatography coupled to fluorescence/mass spectrometry,[22] electrochemistry, particularly enzyme-linked immunosorbent assay (ELISA) etc.[23] Though, still there is a vital need to develop novel detection methods/techniques which can not only perform rapid but also should be simple to use, sensitive and cost-effective for detection of OA in shellfish. Immunosensors are another tool used for detection of OA,23 however, these, require the use of costly antibodies, enzyme and reporter reagents having limited stability and special storage conditions.

Nanotechnology has been widely being utilized in various fields of science such as catalysis, biosensing, optronics and medicinal chemistry. Nanomaterials based biosensors have found extensive use in different areas that not only limit to pathogen detection but play a crucial role in the diagnosis.[24,25] Hence, nanomaterials based biosensors may offer considerable advantages in terms of sensitivity over the currently used techniques. Out of various components employed in biosensors, gold nanoparticles are attracting utmost attention in the area of biomedical research due to their good biocompatibility, significant optical and photothermal properties.[26,27] In addition to this, the surface functionalization of gold nanoparticles is quite simple due to various shapes of gold nanoparticles.[28] The surface functionalization allows us to tune the properties of nanoparticles and widens the region towards various applications.[29]

In this work, we have synthesized a composite to detect OA (Figure 1A) using a naphthalimide based receptor (Figure 1B) and gold nanoparticles. The organic receptor was processed to its nanoparticles (ONPs) (Figure 1C) via reprecipitation method. These ONPS were then coated on gold nanoparticles (Au@ONPs) (Figure 1D) via reported methods (Figure 1E). All the materials prepared were characterised using high resolution transmission electron microscopy (HRTEM), dynamic light scattering (DLS) to check the size and surface morphology. Then composite of both Au@ONPs and ONPs has been prepared which was used to detect okadaic acid. UV – visible absorption spectroscopy, fluorescence spectroscopy and cyclic voltametery techniques were used for the detection of OA.

Experimental

General Information: 1,8-naphthalic anhydride, bromine, 4-picolylamine, 2-fluorophenyl isothiocyanate, chloroauric acid, ascorbic acid and ethylenediamine were purchased from Sigma-Aldrich / local suppliers and were used without further purification. The toxins Okadaic Acid, Domoic acid, Brevetoxin 2, Brevetoxin 3 and Azaspiracids 1 were purchased from Sigma-Aldrich. Milli-Q water (resistivity = 18.2 MΩ.cm, at 25°C) was used to prepare all aqueous solutions. Purified solvents of commercial grade were purchased from Spectrochem. Jeol Instrument was utilized to carry out the ^{1}H NMR and ^{13}C NMR chracterizations, working at 400 MHz for ^{1}H NMR and at 100 MHz for ^{13}C NMR. All chemical shifts were recorded in ppm relative to trimethylsilane as internal reference. The UV – visible absorption spectra were recorded on Shimadzu 2400 spectrophotometer using quartz cuvettes of 1 cm path length. The fluorescence experiments were conducted at room temperature on a Perkin Elmer LS-55 Spectrophotometer with a fixed scanning speed and emission slit width (10 nm). Particle size was determined with dynamic light scattering using the external probe feature of Metrohm Microtrac Ultra Nanotrac particle size analyzer. TEM images were recorded on FEI (Tecnai G2 F-20) instrument that worked at 200 kV and has the resolution of 0.27 nm (point to point). Electrochemical studies were performed using Epsilon BASi instrument at a scan rate of 50.0mV/s. EDAX images were recorded with Jeol JSM-6610LV scanning electron microscope operating at 15 keV.

Synthesis and characterisation of 5: The bromination of 1,8-naphthalic anhydride (8) was done as per method reported in our previous work.[30] In brief, a solution of 1,8-naphthalic anhydride (1.98 g, 10.0 mmol) in KOH (2.8 g in 12 ml water) was prepared and to this solution, 2 ml of bromine was added drop-wise followed by stirring for 30 min at room temperature (Scheme 1). The reaction mixture was then heated to 60 ^{o}C for 6 h. Light brown coloured precipitates separated out on completion of the reaction. The reaction mixture was acidified using hydrochloric acid (HCl) and then filtered the solid residue which was further heated with 5% NaOH solution. The resulted solution was filtered and filtrate was neutralized with diluted solution of HCl. Filtered to collect the solid precipitates and washed it with cold water which resulted into brown powder of 4-bromo-1,8-naphthalic anhydride (7). To synthesize 5; compound 7 (2.77 g, 10 mmol) was dissolved in ethanol and then 4-picolylamine (1.08 g, 10 mmol) was added to it. This solution was refluxed for 8 h and cooled to room temperature on completion of reaction. Precipitates of compound 5 was separated out, filtered and dried as brown coloured powder. Yield = 89%. mp = 167-169 °C. ^{1}H NMR (400 MHz, $CDCl_3$) δ 8.63 (d, J = 4 Hz, 2H, ArH), 8.53 (d, J = 4 Hz, 2H, ArH), 8.26 (d, J = 8 Hz, 2H, ArH), 7.79 (t, J = 8 Hz, 2H, ArH), 7.37 (d, J = 4 Hz, 1H, ArH), 5.37 (s, 2H, picolylamine-CH_2). ^{13}C NMR (100 MHz, $CDCl_3$) δ 150.10, 134.58, 133.35, 131.84, 130.42, 129.56, 127.19, 123.33, 42.73. MS (EI) : *m/z* 367.05 (M^{+}+1).

Synthesis and characterisation of 3: Compound 5 (3.67 g, 10 mmol) was refluxed for 8 h with ethylenediamine (2) (10 mmol) using ethanol as reaction solvent. On completion of reaction, reaction mixture was allowed to cool to room temperature naturally. Yellow coloured compound 3 precipitated out and was filtered and dried. Yield = 82%. mp = 159-161 °C; ^{1}H NMR (400 MHz, $CDCl_3$) δ 8.63 (m, 2H, ArH), 8.53 (dd, J = 1.6 Hz, 2H, ArH), 8.26 (dd, J = 1.6 Hz, 2H, ArH), 7.80 (t, J = 8 Hz, 2H, ArH), 7.34 (dd, J = 8 Hz, 1H, ArH), 5.37 (s, 2H, picolylamine-CH_2), 3.90 (t, J = 4 Hz, 2H, ethylenediamine-CH_2), 3.44 (t, J = 4 Hz, 2H, ethylenediamine-CH_2). ^{13}C NMR (100 MHz, DMSO-d_6) δ 164.43, 163.43, 151.71, 150.15, 147.26, 135.04, 131.69, 129.53, 127.90, 125.05, 122.60, 122.16, 108.03, 104.72, 42.74, 42.38, 38.36. MS (EI) : *m/z* 347.20 (M^++1).

Synthesis and characterisation of 1:

Compound 3 (0.346 g, 1 mmol) was dissolved in dry DCM and to this solution, 2-fluorophenyl isothiocyanate (2) (0.153 g, 1 mmol) was added and reaction mixture was stirred at room temperature for 8 h. On completion of reaction, solvent was evaporated under vacuum. The crude product was then purified using column chromatography to get yellow coloured solid as product 1. Yield = 78%. mp = 187-189 °C. ^{1}H NMR (400 MHz, DMSO-d_6) δ 9.45 (s, 1H, -NH), 8.69 (d, J = 8 Hz, 1H, ArH), 8.43 (dd, J = 1.6 Hz, 1H, ArH), 8.24 (d, J = 8 Hz, 1H, ArH), 8.01 (s, 1H, ArH), 7.95 (s, 1H, ArH), 7.70 (t, J = 8 Hz, 1H, ArH), 7.52 (t, J = 8 Hz, 1H,ArH), 7.23 (dd, J = 8 Hz, 3H, ArH), 7.13 (m, 1H, ArH), 6.95 (d, 1H, ArH), 5.19 (s, 2H, picolylamine-CH_2), 3.82 (t, J = 4 Hz, 2H, ethylenediamine-CH_2), 3.59 (t, J = 4 Hz, 2H, ethylenediamine-CH_2). ^{13}C NMR (100 MHz, DMSO-d_6) δ 182.10, 164.37, 163.38, 151.60, 150.15, 147.31, 135.07, 131.61, 130.18, 129.51, 128.93, 127.89, 124.97, 122.58, 122.15, 120.76, 116.45, 108.02, 104.68, 55.45, 42.92, 42.72, 42.36. MS (EI) : *m/z* 500.19 (M^++1).

Preparation of organic nanoparticles (ONPs)

There are various methods to develop organic nanoparticles; researchers use the method according to their usage. Depending on the fabrication method the properties of the nanoparticles such as size and morphology may vary. The choice of the solvents, temperature and pH govern the fabrication process of the nanomaterials. In present work we have fabricated the ONPs using bottom – up strategy. 1mM solution of the synthesized receptor was prepared in DMSO. The solution was then slowly injected into the water using microsyringe under ultrasonication. The solution was further sonicated for 30 minutes to assure the formation of stable ONPs. This technique is the single step process called re-precipitation. The formation of ONPs was monitored using external probe of a particle size analyzer. Different solvents and concentrations were used to optimize the desirable result. Size distribution of the ONPs was continuously monitored using DLS analysis. TEM analysis was further used to study the size and morphology of the ONPs.

Preparation of Au@ONPs

View Article Online
DOI: 10.1039/D0TB01195A

Gold based organic – inorganic nanohybrid particles have unique synthetic properties. The gold nanoparticles have an absorption maximum near 530 nm, and TEM and DLS experiments were performed for the size and shape of the nanohybrids. Common method used for the fabrication of the nanohybrid[35] uses heating of the solution of ligand and $HAuCl_4$ under rapid stirring, followed by addition of reducing agent like trisodium citrate, sodiumborohydride and ascorbic acid. In present work, we have prepared Au@ONPs via wet chemical method to prepare using ascorbic acid as reducing agents. TEM analysis was further used to study the size and shape of the Au@ONPs. Ascorbic acid solution (0.1 mM) was prepared by dissolving ascorbic acid in type 1 water. Gold solution (0.1 mM) was prepared by dissolving $HAuCl_4$ in water. The required Au@ONPs were prepared by mixing the gold solution, ONPs and ascorbic acid in a ratio of 9:1:9, respectively. Appearance of pink colour confirmed the formation of Au@ONPs. The prepared Au@ONPs were characterized using DLS and TEM analysis.

Chemosensing response of materials:

1mM stock solutions of ONPs and Au@ONPs were prepared in water. A composite solution of ONPs and Au@ONPs was prepared with varied ratios of both materials and the most suitable are achieved with the solution where ONPs:Au@ONPs has ratio of 4:6 by v/v was chosen for further studies. All solutions were shaken properly for a sufficient time and kept undisturbed for 30 min to confirm the homogeneity of solutions, before recording the spectra. The spectroscopic studies were executed at 25 ± 1 °C. ONPs, Au@ONPs and their composite were studies for their interaction with various toxins in aqueous medium. Composite of ONPs and Au@ONPs exhibited tremendous change in the UV-Vis absorption spectra on interaction with Okadaic Acid (OA) as comparative to ONPs and Au@ONPs. Titrations of OA with the composite were done by the addition of successive amounts of OA solution to the composite solution in a 10 mL flask and recording of UV-Vis absorption spectra incremental addition. Similarly, titration experiments of OA with composite were performed in using fluorescence spectroscopy and cyclic voltametery.

Results and discussion

Synthesis and Characterization of materials:

Receptor 1 has been designed with excellent fluorescent properties to target the desired analyte. The synthesis of desired receptor was achieved through the bromination of 1,8-naphthalic anhydride using a method reported in literature.[30] Compound 5 was synthesized by reacting 7 with 1 equivalent of picolylamine in ethanol. After 8 h of refluxing, the reaction mixture was cooled to room temperature, which yielded the brown precipitates of compound 5 (Figure S1-3).

View Article Online
DOI: 10.1039/D0TB01195A

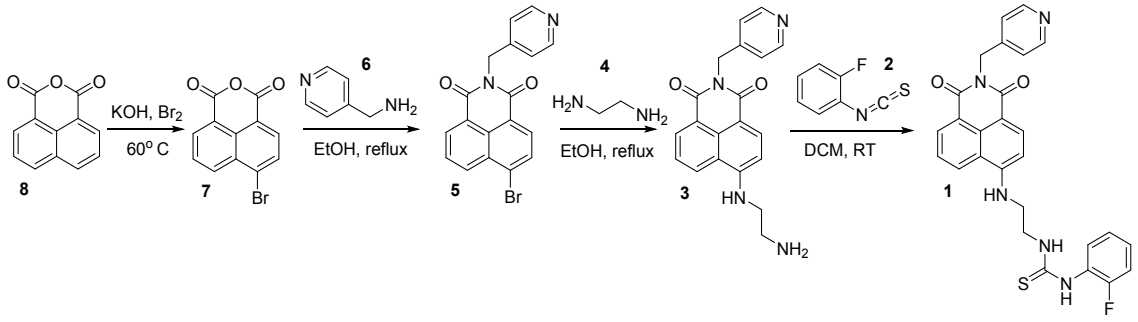

Scheme 1. Synthesis scheme of receptor 1

Compound 3 was synthesized by refluxing 5 with 1 equivalent of ethylenediamine for 8 h, in presence of ethanol. Yellow colored precipitates of compound 3 were separated out on completion of reaction (Figure S4-6). Synthesis of receptor 1 was achieved by reacting compound 3 with 2-fluorophenyl isothiocyanate at room temperature using DCM as reaction solvent. After 8 h, the solvent was evaporated under vacuum to get the crude product which was purified using column chromatography to collect the pure product as yellow solid. Spectroscopic data confirmed formation of receptor 1 (Figure S7-9).

Preparation of organic nanoparticles (ONPs)

Organic nanoparticles and inorganic nanoparticles differ in terms the fabrication principles. Where inorganic nanoparticles are usually prepared by the precipitation of inorganic salt, organic nanoparticles uses number of organic molecules, through self-organization or chemical binding. Formulation of organic nanoparticles (ONPs) requires organic compounds having ability to arrange themselves in a three dimensional system.[31] There are basically two common approaches to synthesize ONPs: "top-down" and "bottom-up" approach. "Top-down" approaches for the synthesis of ONPs, commonly include lithography and mechanical milling. These techniques are quite complicated for use on regular basis as they are not only time consuming but also are energy intensive and have disadvantages like inappropriate control of particle size and introduction of impurities. Due to the tendency of aggregation, "top-down" approach is inappropriate to prepare nanoscale products. Contrary, the bottom-up approach deals with the organized assembly of tiny building blocks, e.g. atomic and molecular aggregates into larger structures (such as organic lattices, clusters, synthesized macromolecules, and supramolecular structures). The "bottom-up" techniques are further classified into two categories viz. re-precipitation and condensation methods. Among these diverse methods, the re-precipitation method has been extensively used for preparation of organic nanoparticles as the factors like shape, size and dispersity can be controlled by altering the condition of reprecipitation.[32] In this method, first the organic compound is completely dissolved in a suitable organic solvent and then this concentrated solution is slowly injected to required anti-solvent under continue sonication. The formation of ONPs is thought to be due to variation in solubility of organic compound in two solvents. Introduction of the organic compound to water surrounding may alter their microenvironment that lead the formation of supramolecular aggregates and formation of nanoparticles by non-covalent molecular interactions (e.g. Vander Waal and л-л interactions).[33,34]

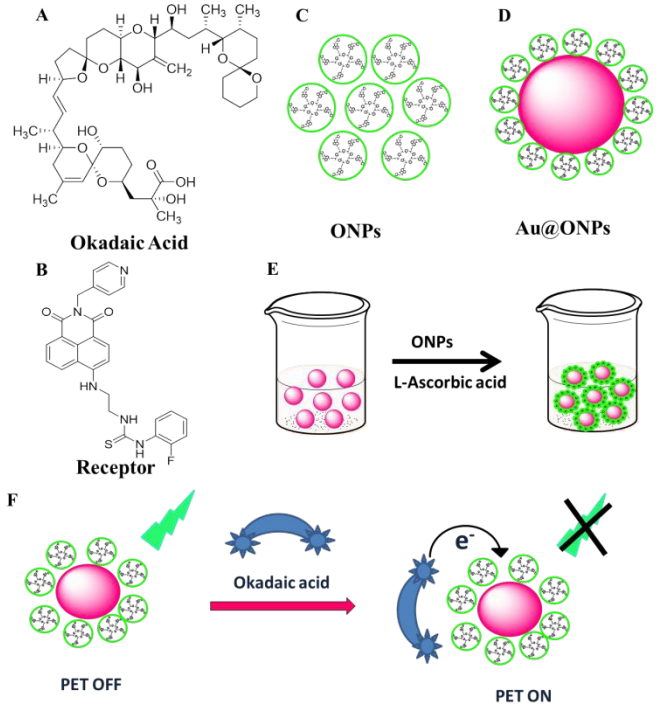

Figure 1 (A) Structure of Okadaic acid (B) Structure of synthesized receptor (C) Representative diagram of ONPs (D) Representative diagram of Au@ONPs (E) Schematic diagram showing the preparation of Au@ONPs and (F) The mechanism for the detection of okadaic acid.

View Article Online
DOI: 10.1039/D0TB01195A

ARTICLE

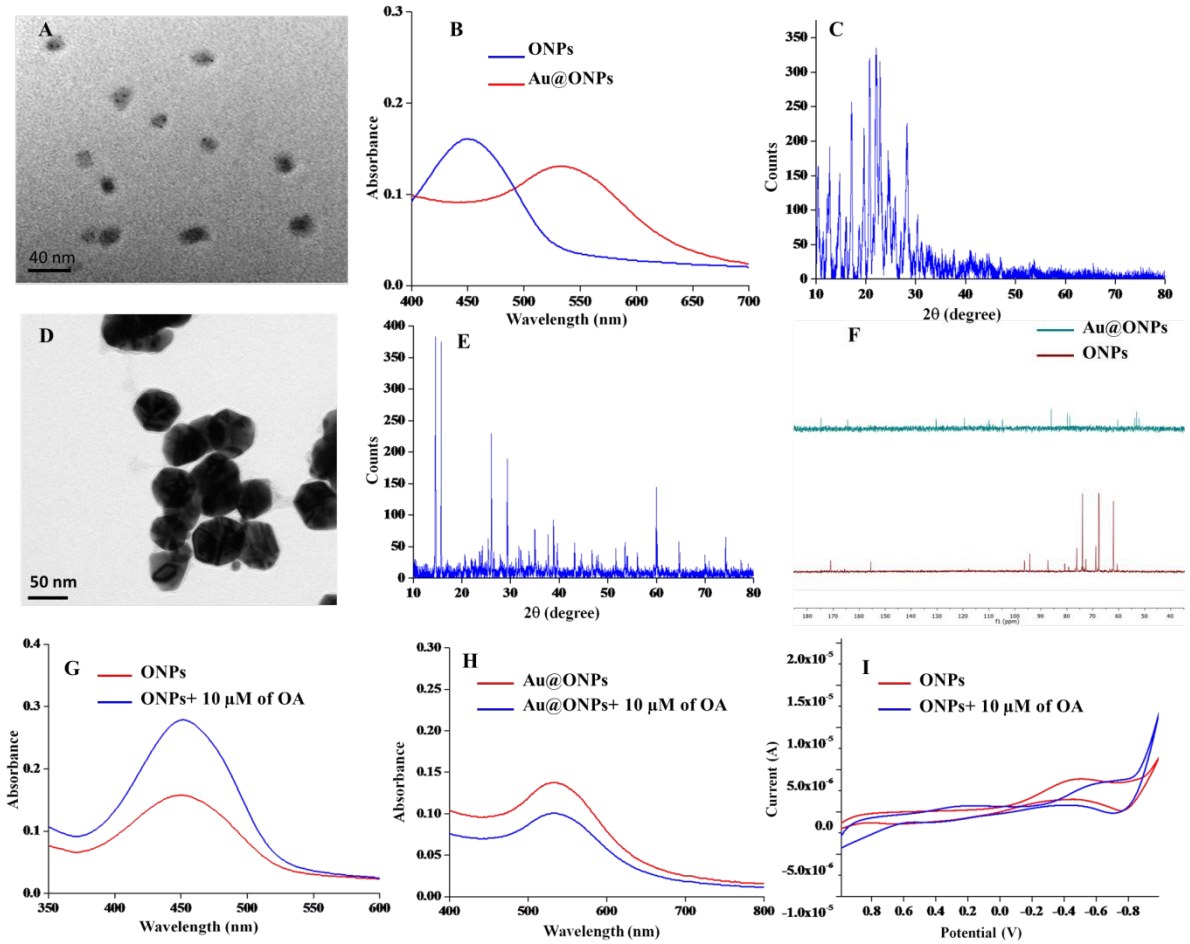

Figure 2 (A) TEM images of ONPs. (B) UV-Vis absorbance spectra of ONPs and Au@ONPs (C) XRD patterns of ONPs (D) TEM images of Au@ONPs (E) XRD patterns of Au@ONPs (F) 13C spectra of ONPs and Au@ONPs (G) Change in UV-Vis absorbance spectra of ONPs on addition of OA (10 µM) (H) Change in UV-Vis absorbance spectra of Au@ONPs on addition of OA (10 µM) and (I) Changes in cyclic voltammetry of ONPs on addition of OA (10 µM).

One can target solid suspensions ranging from 10 nm to 100 nm, using this method. In this work, the compound showed solubility in DMSO over various solvents (DMF, acetonitrile, THF etc.). The synthesized receptor 1 was dissolved in DMSO and with continuous sonication, it was slowly injected into water. The size of the ONPs was confirmed using TEM analysis and it came out to be around 30 nm (Figure 2A). ONPs exhibited absorbance peak at 450 nm (Figure 2B) and λ_{max} at 535 nm (Figure S10). Also, the EDAX analysis data confirmed the presence of carbon, nitrogen, oxygen, fluorine and sulphur (Figure S11). XRD pattern of ONPs are shown in figure 2C.

Preparation of Au@ONPs

The designing of gold coated nanomaterials is interesting part of supramolecular chemistry as it improves the molecular recognition and sensing. For the present work, solutions of ONPs and HAuCl4 were mixed and ascorbic acid was added slowly with continue sonication.[35] The appearance of pink colour validated the formation of gold nanoparticles. TEM analysis showed the size of Au@ONPs to be 40-50 nm (Figure 2D). Further, the formation of Au@ONPs was confirmed with UV-Vis absorption studies which showed the signature peak at 530 nm (Figure 2B) and λ_{max} at 635 nm (Figure S12). To confirm the stability of Au@ONPs with time, samples were kept undisturbed for few days and their UV-Vis absorption studies were carried out. No change in the absorption profile of ONPs confirmed the stability of Au@ONPs. Again, the EDAX analysis

data confirmed the presence of carbon, nitrogen, oxygen and gold (Figure S13). XRD pattern of ONPs are shown in figure 2E. 13C spectra of ONPs and Au@ONPs were also recorded in D_2O (Figure 2F) which show clear shifts in Au@ONPs from ONPs.

Chemosensing response of materials

ONPs of receptor 1 and Au@ONPs were prepared to examine their recognition behaviour towards mycotoxins. The sensing response of ONPs and Au@ONPs over various metal ions (Li^+, Na^+, K^+, Cs^+, Mg^{2+}, Ca^{2+}, Sr^{2+}, Ba^{2+}, Al^{3+}, Cr^{3+}, Mn^{2+}, Fe^{2+}, Co^{3+}, Cu^{2+}, Zn^{2+}, Ag^+, Cd^{2+}, Hg^{2+} and Pb^{2+}), different tetrabutyl ammonium anionic salts (Cl^-, Br^-, F^-, ClO4-, CN^-, NO_3^-, CH_3COO^- and PO_4^-), biomolecules (ATP, ADP, AMP, NADP and NADH) as well as marine toxins (Okadaic Acid, Domoic acid, Brevetoxin 2, Brevetoxin 3 and Azaspiracids 1) was evaluated. All the studies were carried out at 25 ± 1 °C.

Chemosensing response of composite:

In present scenario, various studies have been focused on the synthesis and application of nanoscale materials having unique features owing to their size quantization effects. Gold nanoparticles are attracting the attention, as their colloidal solutions show particular colours as their surface electrons exhibit collective oscillations due to visible light that results in colorimetric change for a variations in the interparticle distance. Particularly, gold nanoparticles when combined with some biomolecules, are supposed to develop new recognition systems for certain reactions between biomolecules and these composites have various applications in biotechnology.[36]

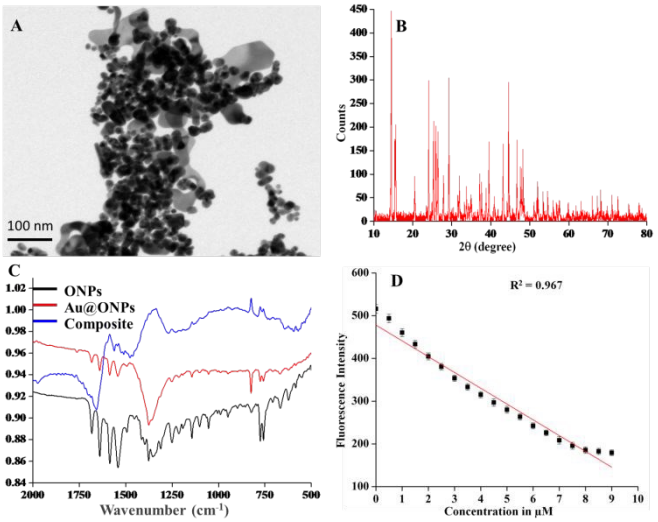

Figure 3 (A) TEM images of composite (B) XRD patterns of composite (C) IR spectra of ONPs, Au@ONPs and composite (D) Linear regression graph between concentrations of OA added to composite.

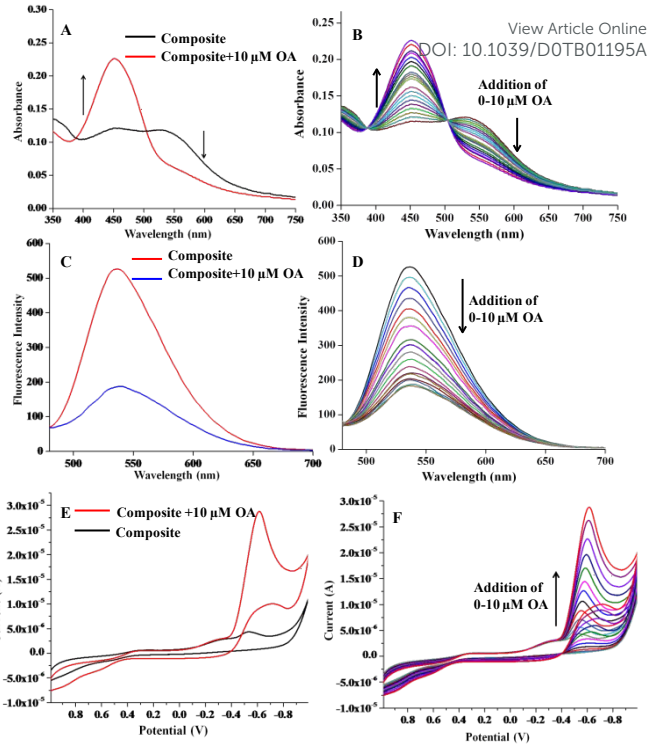

Figure 4 (A) Changes in UV-Vis absorption spectra of composite on addition of OA (10 µM) (B) Changes in UV-Vis absorption spectra of composite on addition successive amounts of OA (C) Change in fluorescent spectra of composite on addition of OA (10 µM) (λ_{ex} = 450 nm) (D) Changes in fluorescent spectra of composite on addition successive addition of OA (λ_{ex} = 450 nm) (E) Changes in cyclic voltammetry of composite on addition of OA (10 µM) (F) Changes in cyclic voltammetry of composite on successive addition of OA.

Reports are present in literature where immunoassays based on the aggregation of gold nanoparticles modified with antibody have been demonstrated by specified binding with an antigen. In another example Mirkin *et al.* demonstrated the polynucleotides detection using specific sequences by enabling the association of gold nanoparticles bearing corresponding nucleotide chains via hybridization with the target polynucleotides.[37] Many other reports are present for detection of heavy metals, antibody and lectin which utilize aggregation of nanoparticles in solutions. Naoki *et al.* have reported a composite of gold nanoparticles and molecularly imprinted polymer as a sensing material having a biomolecule-like activity.[38] Pachfule *et al*. also reported organic – inorganic composite based on gold-nanoparticle for the reduction of nitrophenol.[39] Considering the above discussion, we have thought to prepare a composite material using ONPs and Au@ONPs. To prepare the composite material of ONPs and Au@ONPs, various ratios of both the materials have been prepared and then their UV-Vis absorption and emission profile were tested for the best match. The best results are achieved with the solution where ONPs:Au@ONPs has ratio of 4:6 by volume respectively.

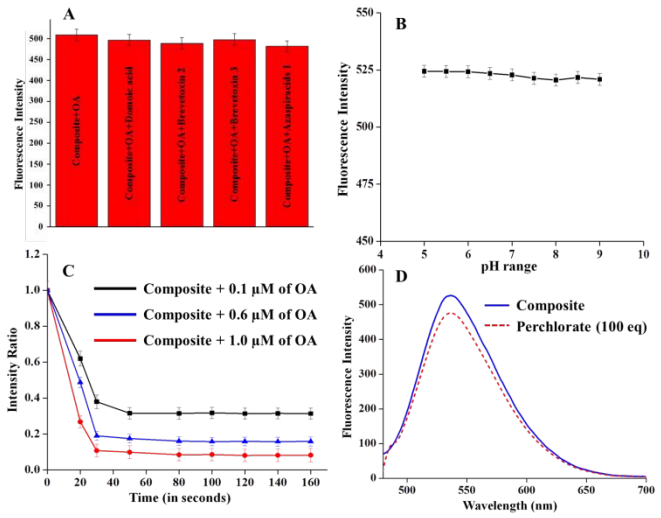

Figure 5 (A) Competitive binding studies of composite containing OA over other selected toxins (B) Effect of pH on fluorescence intensity of composite (C) Plot of the intensity ratio of composite and OA at different concentrations as a function of time in seconds (D) Salt perturbation studies of the composite with the respective fluorescence spectrum recorded upon the addition of 100 equiv of tetrabutyl ammonium perchlorate.

Characterisation of the composite

Once, the ratio of ONPs : Au@ONPs was decided, the composite material was fully characterised using various techniques. Particle size and shape of the composite material was determined using TEM analysis. As is clear from figure 3A, TEM analysis showed different particle sizes of the composite material is 10-40 nm. XRD patterns of composite are shown in figure 3B. A comparison of IR spectra of ONPs, Au@ONPs and composite has been shown in figure 3C.

Chromogenic, fluorescent and electrochemical recognition of okadaic acid:

The recognition behaviour of composite material towards various metal ions (Li^+, Na^+, K^+, Cs^+, Mg^{2+}, Ca^{2+}, Sr^{2+}, Ba^{2+}, Al^{3+}, Cr^{3+}, Mn^{2+}, Fe^{2+}, Co^{3+}, Cu^{2+}, Zn^{2+}, Ag^+, Cd^{2+}, Hg^{2+} and Pb^{2+}), tetrabutyl ammonium anionic salts (Cl^-, Br^-, F^-, ClO_4^-, CN^-, NO_3^-, CH_3COO^- and PO_4^-), biomolecules (ATP, ADP, AMP, NADP and NADH) and marine toxins (Okadaic Acid, Domoic acid, Brevetoxin 2, Brevetoxin 3 and Azaspiracids 1) was evaluated by the addition of the analytes to a fixed amount of composite. The composite exhibited absorption at 450 nm and 530 nm (Figure S15) whereas the fluorescence emission peak displayed at 535 nm. To the fixed volume (5 ml in volumetric flask) of composite solution, 10 µM of each analyte was added. The absorption spectrum depicted weak or insignificant variation in absorption peak when different analytes were added to composite expect Okadaic Acid. A significant change in UV-Vis absorption profile of the composite occurred on addition of Okadaic Acid (Figure 4A). The absorbance peak corresponding to 450 nm showed hyperchromic shift whereas peak corresponding to 530 nm showed quenching and merely disappeared. UV-Vis absorption titrations were performed by gradual addition of Okadaic Acid to the composite solution. Results are plotted in figure 4B. Similarly, addition of 10 µM of Okadaic Acid showed quenching in the fluorescence profile (Figure 4C). To check the binding efficacy of the composite, successive addition of small aliquots of OA to composite solution was done (Figure 4D). This depicted that toxin is binding linearly with composite having a linear regression of 0.967 (Figure 3D). Titrations showed good linearity of about 96.7% in the range (1-8.5 µM). The limit of detection (LOD) of composite can be defined as 3xSD/m, where SD is the standard deviation and m is the slope of the regression line. The detection limit of composite for OA is obtained to be 20 nM. The binding ratio of the nanocomposite with the marine toxin okadaic acid was calculated from Job's Plot. For doing so, intensity ratio of the absorbance (450 nm) was plotted against the [composite]/ [composite + Okadaic Acid]. The stoichiometry of the composite with okadaic acid was found to be 1:1 as shown in figure S18.

Cyclic voltammetric studies (CV) were also carried out for the composite material at a scan rate of 50.0 m where Ag/AgCl was used as reference electrode, Pt disc as working electrode, Pt wire depicted as counter electrode and NaClO4 working as a supporting electrolyte. In case of CV, a shift was observed in cathodic peak, as it changed its position from -0.532 V to -0.618 V with enhancement in current on addition of Okadaic Acid. Similarly, anodic peak showed a change from -0.815 V to -0.847 V with a modulation in the peak (Figure 4E and 4F).

The prime concern about a composite was that it should be selective towards a particular toxin, therefore to check the selectivity towards Okadaic Acid; a competitive binding assay was performed by adding various analytes to the composite solution. To check the selectivity of the composite material, competitive binding test was performed. To perform this study composite solution was taken in different volumetric flasks and then added the 0.5 µM of Okadaic Acid solution to each flask. Then the addition of remaining metal solutions, tetrabutyl ammonium anionic salts, biomolecules and remaining marine toxins to the volumetric flasks was done followed by recording emission spectra for each solution after shaking the solutions. From comparison of emission spectra of composite + OA alone and of composite + OA in the presence of remaining marine toxins (Figure 5A), biomolecules and tetrabutyl ammonium anionic salts (Figure 6) and metal solutions (Figure S17) it was observed that addition of various analytes did not pose any interference to the spectrum and hence the composite can be used for selective determination of Okadaic Acid. The performance of the composite for target analyte may be affected by the pH value of the environment around it due to various reasons. The effect of pH on the emission response of composite was therefore investigated. The experiments were carried out at a pH range from 5.0 to 9.0 (Figure 5B). Both acidic and basic titrations were conducted by changing pH of composite solution using sodium hydroxide and hydrochloric acid and then emission spectra were recorded at various pH values to study the effect of pH on the emission response of host solution. For composite solution, in both acidic (pH<7) and basic conditions (pH>7), the pH has

View Article Online
DOI: 10.1039/D0TB01195A

ARTICLE

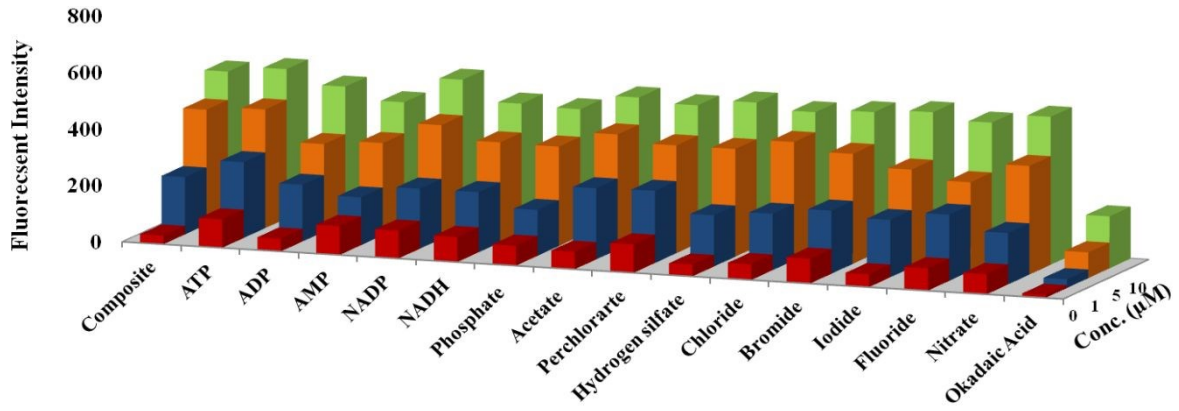

Figure 6 Selectivity test of composite for OA: detection over several analytes. The concentrations of all the compounds are the same, and measurements are performed under identical conditions.

little or no effect on the emission spectra of composite. The fluorescence emission spectrum results revealed that the composite can be used over a pH range from 5 to 9. Besides high selectivity and sensitivity, another necessity for a chemosensor is a short response time to screen the analyte of interest. To examine the response time, fluorescence emission spectra of composite was studied by variation in the concentration of OA in the composite solution. To perform this experiment, composite solution was taken in three volumetric flasks and then different concentration of OA was added to each flask. After fixed intervals of time, the fluorescence spectra of all samples were recorded. The response time of the composite towards OA is concentration-independent, as it was observed that the time required to reach equilibrium does not affect with OA concentrations. In all cases, however, the stable reading could be achieved within 60 seconds after that negligible change in fluorescence intensity was observed (Figure 5C). Thus, the composite can be used for real time monitoring of OA. Similarly to evaluate the effect of salt concentration on fluorescence spectroscopy, increasing concentration of electrolyte i.e. tetra butyl ammonium perchlorate (TBAP), were added to composite solution. It was perceived that even on addition of 100 equivalents of TBAP, fluorescence emission spectra of composite remain almost undisturbed (Figure 5D).

The composite is capable of successful selective and sensitive detection of the marine toxin okadaic acid. The fluorescence quenching is observed due to the photo-induced electron transfer (PET)[40-42] from the okadaic acid to the composite. In the absence of the okadaic acid the electron transfer in inhibited and PET is OFF and high fluorescence is observed. Okadaic acid being electron rich molecule acts as donor and participates in electron transfer process to the HOMO of the nanocomposite and thus quenches the fluorescence intensity. Then mechanism has been shown in the figure 1F.

The detection of okadaic acid was performed in completely aqueous medium. As the ONPs and gold based nano-composite were prepared in water so we have performed the effect of polarity in the presence of DMSO and DMF solvents. As shown in figure S19, we can see that low percentage of DMSO or DMF does not affect the fluorescence profile of the composite's binding with okadaic acid. When the DMSO is more than 12% the fluorescence intensity starts decreasing. Similarly for the DMF, more than 10% of DMF affect the fluorescence profile hence the detection of the okadaic acid.

The figure 6 shows the selectivity of our sensor (composite) over other toxins, anions and biomolecules. These selectivity tests were performed at 0, 1, 5 and 10 μM concentrations of all the analytes. To the solution of okadaic acid, the abovementioned concentrations of the analytes were added and their fluorescence profile was recorded. The results of the figure 6 show that our sensor selectively binds with the sensor and shows quenching of the fluorescence intensity of the composite. Whereas with the rest of the biomolecules such ATP, ADP, AMP, NADP and NADH, composite do not show any changes in the fluorescence intensity hence do not bind with the composite. Similarly, the anions such as phosphate, hydrogen sulphate, chloride, bromide, iodide and nitrate ions do not bind with the composite and no change in the fluorescence profile was observed. These results show the selective binding of the composite with okadaic acid; hence we can successfully say that our fabricated sensor can be used for selective and selective detection of okadaic acid in aqueous medium.

View Article Online
DOI: 10.1039/D0TB01186E

The biological toxicity of our fabricated nano composite was studied by cell viability test with HeLa cells. The HeLa cells were cultured in MEM media with 10 % fetal bovine serum in the presence of 5% carbon dioxide. The incubation of the HeLa cells was carried out at 37°C for 24 hours. The nano composite with and without binding with okadaic acid was incubated with HeLa cells for 24 hours at 37°C and the cell viability was observed. We observed that 90-95 % of HeLa cells recovered from the composite in the absence of okadaic acid. In the presence of composite + okadaic acid the cell viability was found to be 85-90% as shown in the figure S20.

Real Sample Analysis

To investigate the applicability of the sensor in real situation the real sample analysis were carried out. In order to do so the water sample were collected from different sources such as tap water (S1), river water (S2) and Canal Water (S3) were spiked with known concentrations of okadaic acid and explored the sensing capability of the our fabricated nano composite for the sensing of okadaic acid. The table 1 of the real sample analysis is shown below and same has been added to the supplementary information of the manuscript.

Table 1. Real sample analysis of the okadaic acid using our fabricated composite sensor.

Sr. No.	Sample	Conc. of okadaic acid (nM) added	Conc. of okadaic acid (nm) found	% Recovery
1	S1	0	N.D.	N.D.
		25	23.89	95.5
		50	48.69	97.3
2	S2	0	0	N.D.
		25	24.09	96.3
		50	48.9	97.8
3	S3	0	N.D.	N.D.
		25	23.96	95.8
		50	49.01	98

Conclusions

In conclusion, a naphthalimide based receptor was synthesized using the multistep reaction scheme. This fluorescent receptor was then processed into ONPs and Au@ONPs. Binding studies revealed their fair interacting nature towards marine toxin OA but was less sensitive. Fabrication of the composite of Au@ONPs and ONPs modified the sensing properties towards OA and made the sensor much more sensitive and selective for the detection of marine toxin. The limit of detection of the composite was found to be 20 nM. Time response experiment revealed quick binding of the composite with OA, and sensing ability was retained in pH range of 5-9 and also under high salt effects suggesting the workability of the sensor for the detection of OA in real applications.

Conflicts of interest

There are no conflicts to declare.

Acknowledgements

Authors acknowledge Indian Institute of Technology Ropar for providing the infrastructure to carry out the experiments.

References

1 M. Campàs, D. Garibo and B. Prieto-Simón, Analyst, 2012, 137, 1055–1067.
2 M. W. Orner, Mycotoxins in Foodstuff, Springer-Verlag, Berlin, 2007.
3 H. Russmann, ed. 46, 2003, pp. 989–996.
4 A. Molinelli, K. Grossalber, M. Führer, S. Baumgartner, M. Sulyok and R. Krska, J. Agric. Food Chem., 2008, 56, 2589–2594.
5 A. Szkola, E. M. Linares, S. Worbs, B. G. Dorner, R. Dietrich, E. Märtlbauer, R. Niessner and M. Seidel, Analyst, 2014, 139, 5885–5892.
6 V. V. Goftman, N. V. Beloglazova, E. Njumbe Ediage, S. De Saeger, R. Dietrich, E. Märtlbauer and I. Y. Goryacheva, Anal. Methods, 2012, 4, 4244–4249.
7 R. Franz, Defense against toxin weapons, Medical Aspects of Chemical and Biological Warfare, Textbook of Military Medicine, Washington DC, 1997.
8 C. Desmet, L. J. Blum and C. A. Marquette, Anal. Chem., 2012, 84, 10267–10276.
9 European Food Safety Authority, 2008, vol. 589.
10 M. P. D. Jonassen, David, Michael J. Spector, Marcy Driscoll, M. David Merrill, Jeroen van Merrienboer, Handbook of research on educational communications and technology: a project of the association for educational communications and technology., Routledge, 2008.
11 C. E. Stivala, E. Benoit, R. Aráoz, D. Servent, A. Novikov, J. Molgó and A. Zakarian, Nat. Prod. Rep., 2015, 32, 411–435.
12 T. Chen, X. Xu, J. Wei, J. Chen, R. Miu, L. Huang, X. Zhou, Y. Fu, R. Yan, Z. Wang, B. Liu and F. He, PLoS One, 2013, 8, 6–10.
13 M. Taylor, L. McIntyre, M. Ritson, J. Stone, R. Bronson, O. Bitzikos, W. Rourke, E. Galanis, H. Bailey, K. Cordner, M. Feeley, J. Fung, M. Fyfe, K. Hislop, V. Jorgenson, D. Kelly, P. Kendall, D. Moreau, C. Nowakowski, L. Pelletier, H. Swinkels, J. Wong, A. Youssef and S. Zarepourarzil, Mar. Drugs, 2013, 11, 1669–1676.
14 M. Campàs, P. de la Iglesia, M. Le Berre, M. Kane, J. Diogène and J. L. Marty, Biosens. Bioelectron., 2008, 24, 716–722.
15 A. Dounay and C. Forsyth, Curr. Med. Chem., 2012, 9, 1939–1980.
16 V. Meštrović and M. Pavela-Vrančič, Biochimie, 2003, 85, 647–650.
17 Ec, Off. J. Eur., 2004, 69–74.
18 J. Regueiro, A. E. Rossignoli, G. Álvarez and J. Blanco, Food Chem., 2011, 129, 533–540.
19 T. Yasumoto, Y. Oshima and M. Yamaguchi, Nippon Suisan Gakkaishi (Japanese Ed., 1978, 44, 1249–1255.
20 A. Woods and H. Oceanographic, Manual on harmful marine microalgae, 1995.

View Article Online
DOI: 10.1039/D0TB01195A

21 C. Lin, Z. S. Liu, D. X. Wang, H. L. Ren, Y. S. Li, P. Hu, Y. Zhou, Y. P. Guo, X. M. Meng and S. Y. Lu, Anal. Methods, 2014, 6, 7142–7148.
22 R. L. Manger, L. S. Leja, S. Y. Lee, J. M. Hungerforg and M. M. Wekell, Anal. Biochem., 1993, 214, 190–194.
23 A. Hayat, L. Barthelmebs, A. Sassolas and J. L. Marty, Talanta, 2011, 85, 513–518.
24 Z. Liu, Y. Yang, H. Wang, Y. Liu, G. Shen and R. Yu, 2005, 106, 394–400.
25 M. Azimzadeh, M. Rahaie, N. Nasirizadeh, K. Ashtari and H. Naderi-manesh, 2016, 77, 99–106.
26 J. Wang, R. Polsky and D. Xu, Langmuir, 2001, 17, 5739–5741.
27 J. Wang, D. Xu and R. Polsky, J. Am. Chem. Soc., 2002, 124, 4208–4209.
28 Z. Zhu, New Dev. Gold Nanomater. Res., 2016, 43, 95–116.
29 H. Aldewachi, T. Chalati, M. N. Woodroofe, N. Bricklebank, B. Sharrack and P. Gardiner, Nanoscale, 2018, 10, 18–33.
30 M. Verma, N. Kaur and N. Singh, Langmuir, 2018, 34, 6591–6600.
31 D. Horn and R. Jens, Angew. Chem. Int. Ed., 2001, 40, 4330–4361.
32 A. Singh, S. Kaur, N. Singh and N. Kaur, Org. Biomol. Chem., 2014, 12, 2302–2309.
33 M. Wu, X. Xu, J. Wang and L. Li, ACS Appl. Mater. Interfaces, 2015, 7, 8243–8250.
34 A. Kaur, G. Kaur, A. Singh, N. Singh and N. Kaur, ACS Sustain. Chem. Eng., 2016, 4, 94–101.
35 Monika, N. Singh, J. R. Ascenso and P. M. Marcos, Supramol. Chem., 2019, 31, 313–321.
36 L. Sun, K. Bin Sung, C. Dentinger, B. Lutz, L. Nguyen, J. Zhang, H. Qin, M. Yamakawa, M. Cao, Y. Lu, A. J. Chmura, J. Zhu, X. Su, A. A. Berlin, S. Chan and B. Knudsen, Nano Lett., 2007, 7, 351–356.
37 N. L. Rosi, D. A. Giljohann, C. S. Thaxton, A. K. R. Lytton-Jean, M. S. Han and C. A. Mirkin, Science (80-.)., 2006, 312, 1027–1030.
38 J. Matsui, K. Akamatsu, S. Nishiguchi, D. Miyoshi, H. Nawafune, K. Tamaki and N. Sugimoto, 2004, 76, 1310–1315.
39 P. Pachfule, S. Kandambeth, D. D. Diaz and R. Banerjee, 2014, 3169–3172.
40 C. A. Huerta-Aguilar, T. Pandiyan, N. Singh, and N. Jayanthi, Spectrochimica Acta Part A: Molecular and Biomolecular Spectroscopy, 2015, 146, 142-150.
41 C. A. Huerta-Aguilar, B. Ramírez-Guzmán, T. Pandiyan, J. Narayanan, and N. Singh, Photochemical & Photobiological Sciences, 2019, 18(7), 1761-1772.
42 D. S. Huerta-José, J. G. Hernández-Hernández, C. A. Huerta-Aguilar, T. Pandiyan, Sensors and Actuators B: Chemical, 2019, 293, 357-365.

View Article Online
DOI: 10.1039/D0TB01195A

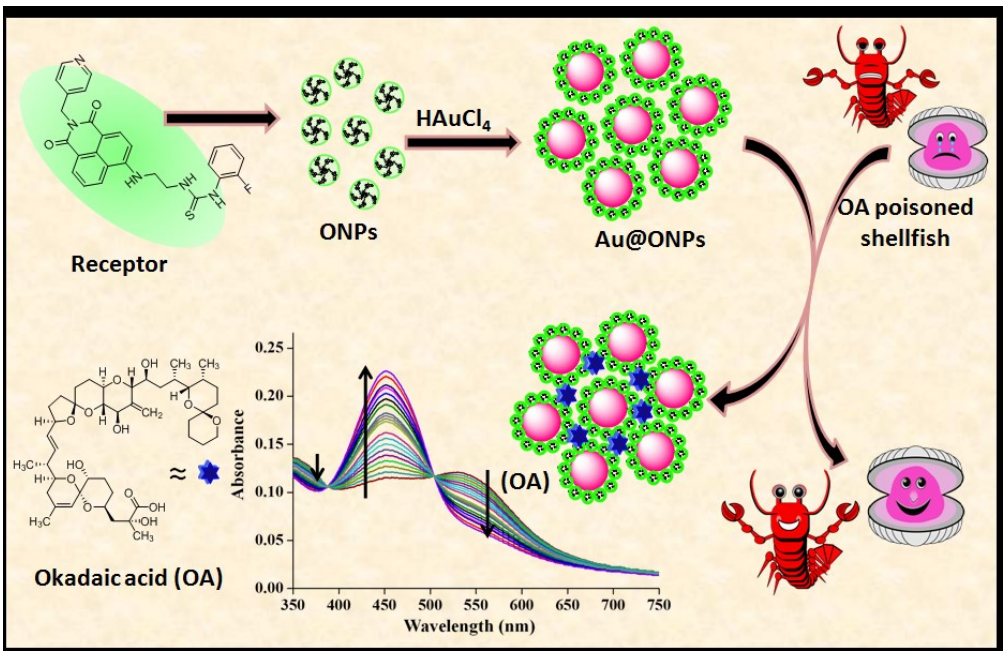

246x159mm (96 x 96 DPI)